Super-compressible DNA Nanoparticle Lattices

Sunita Srivastava,[a] Dmytro Nykypanchuk,[a] A.Tkachenko,[a] Mathew M Maye,[b] and Oleg Gang,[*a]

[a]*Center for Functional Nanomaterials, Brookhaven National Laboratory, Upton, NY, 11973.*

[b]*Department of Chemistry, Syracuse University, Syracuse, NY, 13244.*

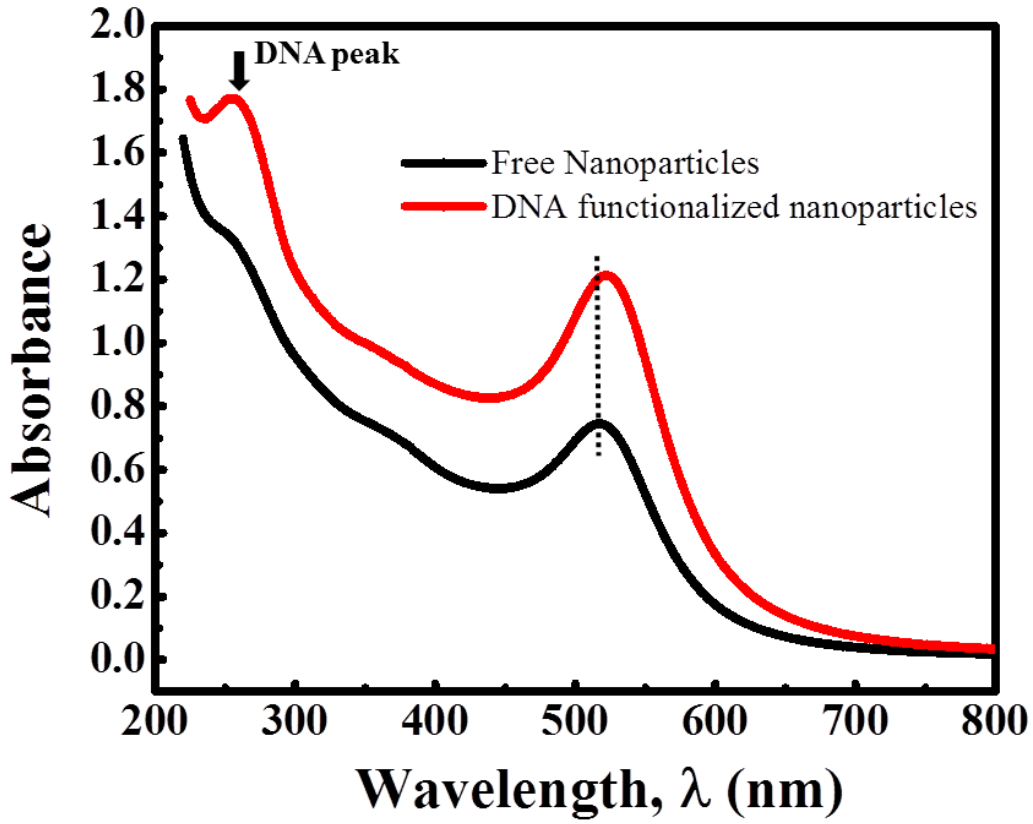

Figure S1: UV- vis spectra of free gold nanoparticles (black) and DNA functionalized NP (red) collected on Perkin-Elmer Lambda 35 spectrometer (200nm- 800nm). The peak at 256nm (arrow) in the red curve is due to the attachment of DNA chains on the NP surface. The red shift of ~ 5nm in the absorbance maxima were also observed due to attachment of DNA chains.

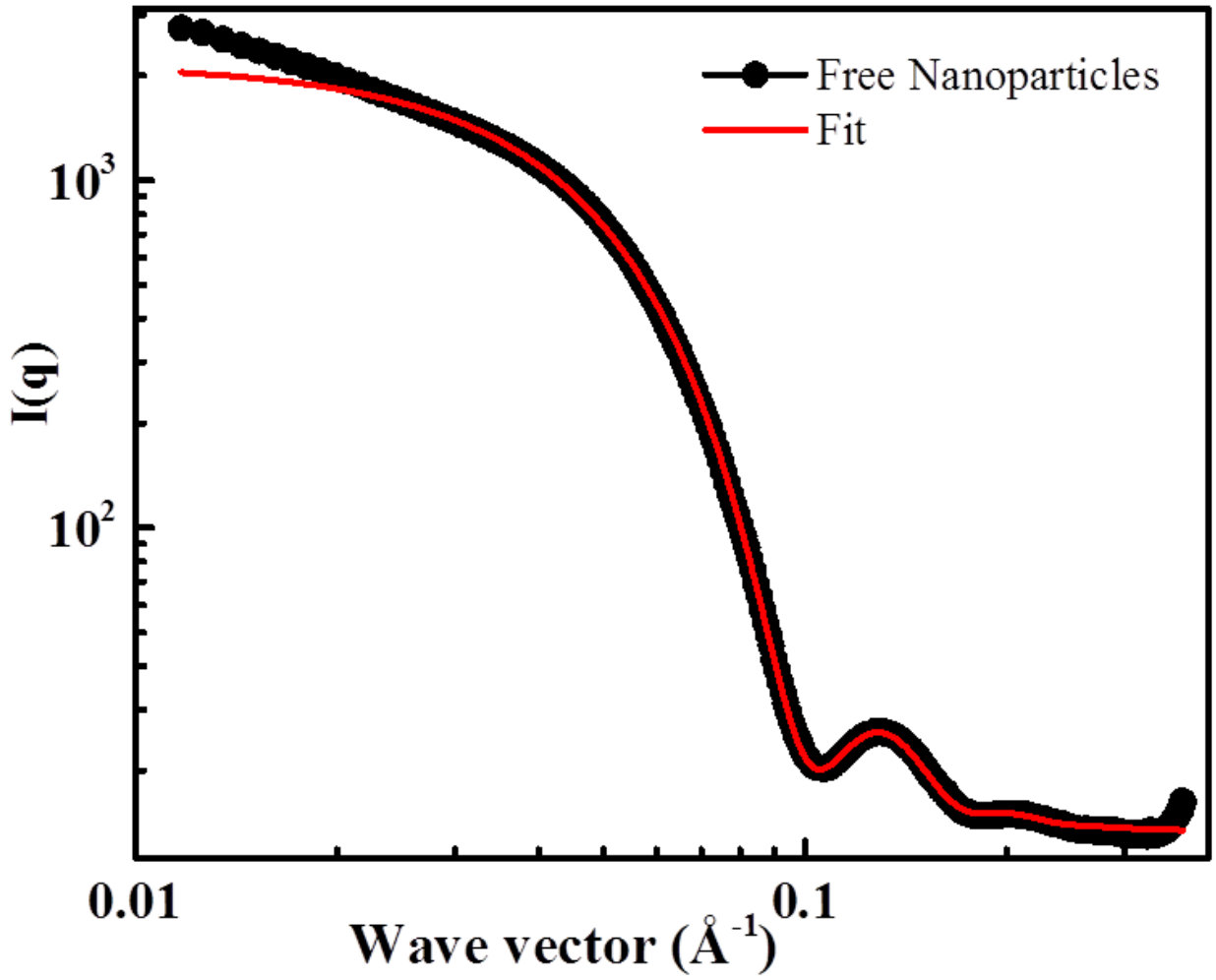

Figure S2: Scattering intensity from free gold nanoparticles (black) before functionalization with ssDNA and the corresponding fit (solid red line) using spherical form factor of particles. The particles sizes were estimated as 9.8 nm ± 0.6 nm using Gaussian distribution for the particle size. We used Irena: tool suite for modeling and analysis of small-angle scattering (http://usaxs.xray.aps.anl.gov/staff/ilavsky/irena.html) (1).

Table S1: The DNA sequence design (5' to 3') for systems presented in paper. HSC_6H_{12} represents the thiol modification. [*k*]' denotes the complementary DNA sequence. DNA strands, "*m*" - 29, 20 and 9 were added to flexible systems, *n*-[*k*] to obtain semi-rigid systems (*n*-*m*-[*k*]) as described in the main text.

Flexible systems : *n*-[*k*]	
50-[15]	HSC_6H_{12}-TTTTTTTTTTTTTTTTTTTTTTTTTTTCGTTGGCTG GATAGCTGTGTTCTTAACCTAACCTTCAT
50-[15]'	HSC_6H_{12}-TTTTTTTTTTTTTTTTTTTTTTTTTTTCGTTGGCTG GATAGCTGTGTTCTATGAAGGTTAGGTTA
35-[15]	HSC_6H_{12}-TTTTTTTTTTTTCGTTGGCTGGATAGCTGTGTT CTTAACCTAACCTTCAT
35-[15]'	HSC_6H_{12}-TTTTTTTTTTTTCGTTGGCTGGATAGCTGTGTTCTA TGAAGGTTAGGTTA
15-[15]	HSC_6H_{12}-TTTTTCGTTGGCTGTTAACCTAACCTTCAT
15-[15]'	HSC_6H_{12}-TTTTTCGTTGGCTGTATGAAGGTTAGGTTA
20-[10]	HSC_6H_{12}-TTTTTCGTTGGCTGTTAACCTAACCTTCAT
20-[10]'	HSC_6H_{12}-TTTTTCGTTGGCTGT TAACCATGAAGGTTA
DNA sequence for Semi- rigid systems: *n*-*m*-[*k*]	
DNA strand-29 (m)	GAACACAGCTATCCAGCCAACGAAAAAAA
DNA strand-20 (m)	GAACACAGCTATCCAGCCAA
DNA strand -9 (m)	CAGCCAACG

Table S2: Compression factor obtained from ratio of lattice constants, $\frac{a_o}{a}$ and corresponding ratio for volume, $\frac{V_o}{V}$ for different flexible systems (left) and semi-rigid systems (right). The compression factors are calculated with reference to lattice constant at PEG concentration of 30 *wt%* for all the systems.

Systems	$\frac{a_o}{a}$	$\frac{V_o}{V}$
50 - [15]	1.58	3.94
35 - [15]	1.43	2.92
15 - [15]	1.32	2.29
20 - [10]	1.30	2.19

Systems	$\frac{a_o}{a}$	$\frac{V_o}{V}$
20 - 29 - [15]	1.79	5.74
29 - 20 - [15]	1.77	5.54
05 - 29 - [15]	1.65	4.49
14 - 20 - [15]	1.62	4.25
10 - 09 - [10]	1.26	2.00

PEG penetration

The penetration of the PEG molecules in the crystallites strongly depends on a mesh size of DNA networks and it varies for different systems due to DNA length. The PEG penetration into the DNA-reach region of the DNA-NP superlattice is determined by an entropic barrier that is associated with confinement of PEG chains in a void formed by DNA matrix, so called mesh size ξ. In order to estimate it, consider the surface of a Wigner-Seitz cell of a given particle in the superlattice. By approximating it as a sphere, we can estimate its overall area as πa^2 (a is center-to-center distance of the neighboring particles). This surface is intersected by $M \approx 50$ DNA chains for our particles. We can now determine the local mesh size ξ as the radius of a spot that in average contains one chain: $\pi M \xi^2 = \pi a^2$, therefore $\xi \approx a/\sqrt{M}$. Note that this result is purely geometric, and does not rely on any particular physical model of DNA. Since the gyration radius of the used PEG molecules is about 8.6 nm, no significant PEG penetration is expected when $a < R_{PEG}\sqrt{M} \approx 60\, nm$. For our sample with the largest "*h*" (see Fig. 3, about 22nm) a center-to-center distance is about 33nm, i.e. significantly below 60 nm, hence a PEG penetration is not expected. In order to verify the validity of our estimations we have designed a system with a larger lattice constant, a is about 53nm, for which the corresponding mesh size is about 7.5nm. For this system we have conducted similar compression experiments. We found the evidence of PEG penetration for system with a=53nm at low osmotic pressures: the lattice constant changes very little with the PEG concentration increase. This indicates that indeed when the mesh size is comparable with the PEG radius of gyration there is a more complicated dependence on the osmolyte concentration. The systems with penetrating PEG behavior were not including in the presented study.

Theory: Ideal chain confined in a spherical shell.

Here we solve the problem of an ideal polymer chain confined in a spherical shell, with two ends of the chains attached to the internal and external surfaces of the shell, respectively. This geometry models the situation in DNA-nanoparticle superlattices, with the spherical shell representing the Wigner-Seitz cell of a given particle.

The problem can be solved by using the well-known mapping of the ideal polymeric chain problem onto diffusion (or Schrödinger) equation [2]. Specifically, since the ideal chain follows a random walk statistics, its probability distribution function can be obtained by solving the following equation:

$$\left[\frac{\partial}{\partial s} - \frac{l_p}{3}\Delta_r\right] G(\vec{r},\vec{r}',s) = \delta(\vec{r},\vec{r}')\delta(s) \qquad \text{(S1)}$$

Here $G(\vec{r},\vec{r}',s)$ is the Green function which represents the probability of finding the two ends of a chain segment of length s in points $\vec{r}$ and $\vec{r}'$, respectively. For the spherical with inner and outer diameters d and $d+h$, respectively, we need to solve this equation with zero boundary conditions at both surfaces:

$$G(\vec{r},\vec{r}',s) = 0, \quad for \;\; |\vec{r}| = \frac{d}{2}, |\vec{r}| = \frac{d+h}{2}, \left|\overrightarrow{r'}\right| = \frac{d}{2}, \; or \;\; \left|\overrightarrow{r'}\right| = \frac{d+h}{2} \qquad \text{(S2)}$$

Since the Green function is proportional to the number of trajectories leading from given initial to final point, it is proportional to the partition function of the confined chain. Because of the zero boundary conditions, we cannot assume the initial and final points to be exactly on the interfaces of the confinement region. Instead, we need to find the value of $G(\vec{r},\vec{r}',L)$ for $|\vec{r}| = \frac{d}{2} + \varepsilon$ and $\left|\overrightarrow{r'}\right| = \frac{d+h}{2} - \varepsilon$, where ε is sufficiently small length, and L the total contour

length of the chain. The spherically symmetric solution to the diffusion equation with the above zero boundary conditions can be written as

$$G(r,r',s) = \frac{1}{\pi r r' h}\sum_{n=1}^{\infty} \sin\left(\frac{\pi n(2r-d)}{h}\right) \sin\left(\frac{\pi n(2r'-d)}{h}\right) \exp\left(-\frac{l_p s}{3}\frac{\pi^2 n^2}{h^2}\right) \quad \text{(S3)}$$

By integrating G over two spherical surfaces, $|\vec{r}| = \frac{d}{2} + \varepsilon$ and $\left|\overrightarrow{r'}\right| = \frac{d+h}{2} - \varepsilon$, we can calculate the partition function of the confined chain:

$$Z = (4\pi r' r \varepsilon)^2 \frac{\partial}{\partial r}\frac{\partial}{\partial r'} G(\vec{r},\vec{r}',L)\Big|_{|\vec{r}|=\frac{d}{2};\ |\overrightarrow{r'}|=\frac{d+h}{2}} \quad \text{(S4)}$$

The resulting free energy per chain, $F = -kT\log \mathrm{Z}$:

$$F = -kT \log\left[\frac{(\mathrm{d+h})}{\mathrm{h}^3}\sum_{n=1}^{\infty}(-1)^n n^2 \exp\left(-\frac{l_p L}{3}\frac{\pi^2 n^2}{h^2}\right)\right] + const \quad \text{(S5)}$$

This is the exact result for the spherical geometry, i.e. Eq. (1) of the main text.

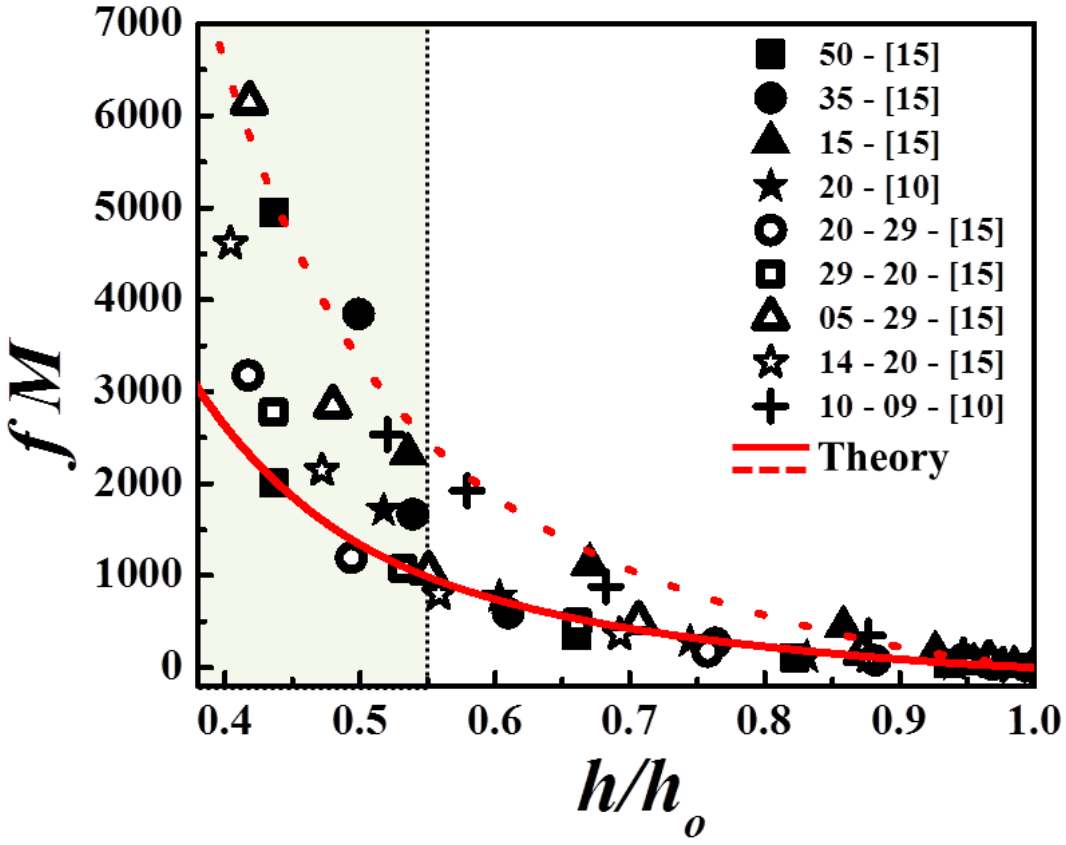

Figure S3: The total compression force, *fM*, plotted for all the different systems vs molecular deformation, h/h_o. Solid and dashed lines were obtained using eq (7) as discussed in the main text. Complete range of *fM* vs h/h_o are presented. The shaded dashed region marks h/h_o < 0.55 where deviation of the theory from the experimental data are observed. At high compressions, excluded volume becomes important, the effect that is not incorporated in the theory.

References:

1. J. Ilavsky and P. R. Jemian**,** *J. Appl. Cryst.* **42(2),** 347-353, (2009).

2. A. K. Dolan and S. F. Edwards, *Proc. R. Soc. London A* **337**, 509 (1974).